# On Manoeuvrability of Semi-Displacement Craft in Astern Seas

Evren Armaoğlu, *Department Universities of Strathclyde and Glasgow*

Zafer Ayaz, *Universities of Strathclyde and Glasgow*

Dracos Vassalos, *Universities of Strathclyde and Glasgow*

Toru Katayama, *Osaka Prefecture University*

**ABSTRACT**

The motions of semi-displacement ships travelling in astern seas are investigated. The focus is on the vertical dynamic forces which should not be neglected at this speed range. A database of dynamic forces acting on the ship depending on the running attitude and speed of the ship is measured from fully captive model experiments and used to characterize their effect on numerical simulations. A manoeuvring mathematical model using horizontal body axis, which allows for a combination of seakeeping and manoeuvring models, taking into account high-amplitude motions and memory effects, is used and the forces and motions are evaluated in six degrees of freedom in time domain. The results are validated with semi-captive model experiments in waves for regular following seas in three degrees of freedom. The effect of speed on transverse stability is discussed.

**Keywords:** *Semi-displacement, Astern seas, Manoeuvring*

## 1. INTRODUCTION

Over the last forty years, the number of High-Speed Craft (HSC) has increased exponentially. The increasing demand for speed in marine surface vehicles, combined with the technological advances have resulted in the development of large HSC, capable of carrying large number of passengers and cargo (Ritter & Templeman, 1998). Due to economical interests the general type of research for these kind of ships are mainly focused on propulsion, machinery, lightweight materials and hydrodynamically efficient hull forms. However if safety is of prime importance when designing, building and operating HSC, the dynamic behaviour in a seaway must be assessed properly.

There is an increased awareness of safety in marine community and the types of dangerous situations a ship may be subject to are well defined. Anecdotal evidence of the way in which HSC behave in conditions such as surf-riding, broaching and bow-diving has given cause for concern in relation to passenger safety (BMT, 2003). For astern seas, benchmarks are set by ITTC based on experiments with a fishing vessel and a container both displacement ships (ITTC, 2002). Focus of these experiments were unstable phenomena like parametric-roll, surf-riding and broaching. The critical speed was defined as approximately Froude number 0.4 in pure following seas where the wave is travelling with the ship. It is reasonable to think that this is the most dangerous situation for a ship especially if travelling on a wave crest where transverse stability is greatly reduced. What has not been included by many is the effect of dynamic forces as the speed increases.

While the dynamic stability for displacement ships are concentrated on horizontal motions, for high speed craft the initial interest was for planing craft and vertical motions. This is because the interest in high speed sea craft has started with the seaplanes that can land to sea with very high speed. The impact force applied to the seaplane floats during landing was a concern first as a structural problem (Von Karman, 1921). Later the problem turned to deal with the porpoising phenomenon, which is a coupled pitch and heave motion that can be seen in high speed at sea (Martin, 1978). As the problem turned to ship motions as propulsion mechanisms allowed ships to travel in those speed regions, additional problems such as corkscrew were seen (Katayama, 2002).

Because of navy's demand for high speed displacement ships, couple of series research were performed in different countries and the well known Series 64 and NPL series were born (Yeh., 1965, Bailey., 1976). It was with the NPL series that the speed induced instability non-zero heel was reported and interest in roll-induced instability for high speed craft began (Marwood & Bailey., 1968).

Baba, Asai & Toki (1982) used a sway-yaw-roll coupled motion model to investigate roll-induced instabilities of high-speed semi-displacement crafts and compared simulations with experiments. They found that GM/U rather than the hull forms has a major effect on the roll-induced instability at high speeds.

Codega & Lewis (1987)'s case study of a planing hull that goes unstable at high speed unlocked many of the reasons why many unstable phenomena happen at high speeds. They referred to Yegorov et al. (1981) and stated that until a high-speed boat reaches a purely planing region the stability of the hull will decrease from the static case. This is because the static hydrodynamic forces have decreased but the planing pressures have not been developed at the bottom. Codega has underlined a very good point that although the studies for high-speed hulls are made for prismatic hulls only, which have constant deadrise angle, this is not the case for a practical boat. Although the bottom pressures for prismatic craft are well defined, the bottom pressures for craft with varying deadrise angle are unknown. They performed systematic experiments in full-scale to measure these pressures. In the end they recommended that a naval architect should avoid a high-speed, round bilge boat with any appreciable amount of deadrise because it will become transversely unstable if driven fast enough.

The concentration of the major studies being for head sea calculations is a very convenient one because as the speed increases to the planing range the encounter frequency in following waves become negative and the ship starts overtaking the waves. This however happens generally after Froude number 0.7 where the craft has already developed a running attitude due to speed. The effect of the running attitude on transverse stability for this speed region and heading in waves is, to the author's knowledge, uninvestigated.

The aim of this paper is to probe deeper to the already known following seas instabilities by focusing on the effects of vertical motions and speed on the transverse characteristics of the hull. An existing numerical program is further developed to include the effect of dynamic forces. Experiments are performed following Ikeda et. al. (1993) to obtain a database of hydrodynamic forces by fully captive model experiments. Vertical motions in regular waves are also measured by semi-captive tests to validate the numerical results.

## 2. MATHEMATICAL MODEL

The equations of motion are presented with respect to horizontal body axes. External forces are described with respect to this axis system in the right hand side of the equations of motion. The ship is assumed as a rigid body having six degrees of freedom with no restriction on motion amplitudes.

The relationships between coordinate systems are shown in Fig. 1. It is seen that in deriving the basic equations of motion, we make use of three different coordinate systems. First is an earth fixed system $O-\xi\eta\zeta$. The second is the general body axes which is fixed in the ship and the origin $G$ located at the center of gravity of the ship defined by $G-xyz$. The third is the horizontal body axes fixed in the ship with origin at $G$ defined by $G-x'y'z'$.

In Fig. 1, $x$, $y$, $z$ represent kinematics; $u$, $v$, $w$ are linear velocities; $p$, $q$, $r$ are angular velocities; and $\varphi$, $\theta$, $\psi$ are Euler angles of rotations. Newton's second law describes the equation of motion for a ship having six degrees of freedom and under the action of certain external forces. The representation of equations of motion in horizontal body axes are derived in previous studies (Hamamoto & Kim, 1993 and Ayaz, 2003).

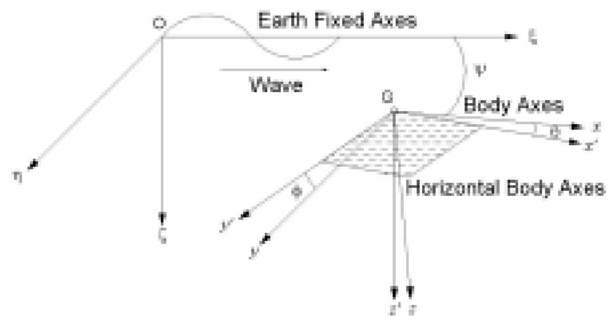


Figure 1. Systems of Coordinates

The generalized form of equations of motion is as follows:

$$
\begin{aligned}
&m(\dot{V}_G+\omega\times V_G)=F\\
&H_G+\omega\times H_G=G
\end{aligned}
\tag{1}
$$

where $m$ is the mass of the ship, $H_G$ is the momentum about the center of gravity, $\omega$ angular velocity, $V_G$ linear velocity and $F$ and $G$ are the sum of all forces and moments acting on the ship respectively. The resultant equations are as follows considering force and moment components:

$$
\begin{aligned}
&\mathrm{m}(\dot{\mathrm{U}}-\mathrm{VR})=\mathrm{X}'\\
&\mathrm{m}(\dot{\mathrm{V}}+\mathrm{UR})=\mathrm{Y}'\\
&\mathrm{m}\dot{\mathrm{W}}=\mathrm{Z}'+\mathrm{mg}
\end{aligned}
\tag{2}
$$

$$
\begin{aligned}
&\left(\mathrm{I}_{yy}-\mathrm{I}_{xx}\right)\left[\sin 2\theta\left(\mathrm{QP}+\frac{1}{2}\dot{\mathrm{R}}\right)+\cos 2\theta\,\mathrm{QR}\right]\\
&+\left(\mathrm{I}_{xx}\cos^2\theta+\mathrm{I}_{yy}\sin^2\theta\right)\dot{\mathrm{P}}-\mathrm{I}_{yy}\mathrm{RQ}=\mathrm{K}'\\
&\left(\mathrm{I}_{yy}-\mathrm{I}_{xx}\right)\left[\sin 2\theta\left(\frac{1}{2}\mathrm{R}^2\right)\right]\\
&+\left(\mathrm{I}_{xx}\cos^2\theta+\mathrm{I}_{yy}\sin^2\theta\right)\mathrm{RP}+\mathrm{I}_{yy}\dot{\mathrm{Q}}=\mathrm{M}'\\
&\left(\mathrm{I}_{xx}-\mathrm{I}_{zz}\right)\left[\sin 2\theta\left(\mathrm{QR}-\frac{1}{2}\dot{\mathrm{P}}\right)-\cos 2\theta\,\mathrm{QP}\right]\\
&+\left(\mathrm{I}_{xx}\sin^2\theta+\mathrm{I}_{zz}\cos^2\theta\right)\dot{\mathrm{R}}=\mathrm{N}'
\end{aligned}
\tag{3}
$$

where, $\mathrm{X}', \mathrm{Y}', \mathrm{Z}', \mathrm{K}', \mathrm{M}'$ and $\mathrm{N}'$ are surge, sway, heave, roll, pitch and yaw external forces and moments composed of forces due to waves, speed and control systems. U, V, W are surge, sway and heave linear velocities; Q, P, R are roll, pitch and yaw angular velocities in the horizontal body axes system; $\mathrm{I}_{xx}, \mathrm{I}_{yy}, \mathrm{I}_{zz}$ are roll, pitch and yaw moment of inertias respectively. The external forces and moments in equations of motion are represented as follows:

$$
\begin{aligned}
&\mathrm{X}'=-\iint_s p\mathbf{n}_X\,dS+\mathrm{X_H}+\mathrm{X_P}+\mathrm{X_S}\\
&\mathrm{Y}'=-\iint_s p\mathbf{n}_Y\,dS+\rho U\int_{\Gamma_x}\Phi_D\mathbf{n}_Y\,dS+\mathrm{Y_H}+\mathrm{Y_S}\\
&\mathrm{Z}'=-\iint_s p\mathbf{n}_Z\,dS+\rho U\int_{\Gamma_x}\Phi_D\mathbf{n}_Z\,dS+\mathrm{Z_H}+\mathrm{Z_D}\\
&\mathrm{K}'=-\iint_s p(\mathbf{r}\times\mathbf{n}_{YZ})\,dS+\rho U\int_{\Gamma_x}\Phi_D(\mathbf{r}\times\mathbf{n}_{YZ})\,dS\\
&+\mathrm{K_H}+\mathrm{K_S}\\
&\mathrm{M}'=-\iint_s p(\mathbf{r}\times\mathbf{n}_{ZX})\,dS+\rho U\int_{\Gamma_x}\Phi_D(\mathbf{r}\times\mathbf{n}_{ZX})\,dS\\
&+\mathrm{M_H}+\mathrm{M_D}\\
&\mathrm{N}'=-\iint_s p(\mathbf{r}\times\mathbf{n}_{XY})\,dS+\rho U\int_{\Gamma_x}\Phi_D(\mathbf{r}\times\mathbf{n}_{XY})\,dS\\
&+\mathrm{N_H}+\mathrm{N_S}
\end{aligned}
\tag{4}
$$

Here the first terms on the right hand side of the equations represents the incident wave forces and moments, including hydrostatic forces, where $p$ is the pressure evaluated at the instantaneous hull surface, $\mathbf{n}$ is the normal vector and $\mathbf{r}\times\mathbf{n}$ is the vector fixed with respect to the center of gravity (Hamamoto & Kim, 1993). The second terms are diffraction forces which are obtained as disturbance forces using Ohkusu (1986)'s low encounter frequency slender body theory, where $\Phi_D$ is the disturbance due to waves and $\Gamma_x$ denotes integration over section contour to the still water surface. Diffraction force in surge is ignored because the incident wave force is dominant. For the rest of the forces, subscript H indicates manoeuvring (hull) forces, P indicates forces due to propulsion mechanism, S indicates forces due to steering mechanism and D indicates dynamic forces due to speed.

The implementation of dynamic forces can be done by either direct calculation methods or from a database containing the necessary force and moment components obtained from either experiments or a calculation procedure such as a CFD methodology. The method of calculation for propulsion and steering system varies depending on the system being a propeller-rudder combination, azimuthing pod drive or a waterjet. For convenience MMG model is used in the calculations. Wind forces and ride control systems can also be added but are left out for the initial study.

The detailed descriptions of the mathematical model in whole were given in numerous previous studies (Ayaz et. al., 2002, Ayaz., 2003, Ayaz, Vassalos, Turan, 2006). The only addition here is the dynamic forces due to speed. The non-linear equations (2) and (3) can be expressed in matrix form representing displacements, velocities and accelerations in the following form;

$$\begin{aligned}&(M+A)\ddot{X}(t)+B\dot{X}(t)+CX(t)\\&=F(\varsigma_w, X(t), \dot{X}(t), \ddot{X}(t))\end{aligned} \tag{5}$$

where $X$ is the solution vector to the equations of motion, $M$ is the inertia matrix, $A$ is the added mass matrix, $B$ is the damping matrix, C is the restoring coefficient matrix and F is the external force matrix where $\varsigma_w$ is the wave profile which can be represented as regular or long crested irregular seas.

According to previous studies the most dangerous situations the ship is going to be in are in regular waves, followed by long crested irregular waves. Short crested waves are the least likely for unstable behaviour leading to capsize (ITTC, 1999).

The equations (5) are solved in time domain via Fourth Order Runge-Kutta algorithm. In order to evaluate the frequency dependence of the hydrodynamic coefficients impulse response functions are implemented in the numerical model. Since the computations are done in time domain they are represented by convolution integrals. Following Cummins (1962)'s work, radiation forces in time domain is represented as :

$$\begin{aligned}&F_{ij}=-a_{ij}(\infty)\dot{V}_j-\int_0^\infty K_{ij}(t)V_j(t-\tau)d\tau\\&i,j=1,2,3,4,5,6\end{aligned} \tag{6}$$

where the first term is the infinite frequency added mass and the second term is the impulse response function. Kernel function $K_{ij}(t)$ is represented as the frequency domain damping function in the following form:

$$\begin{aligned}&K_{ij}(t)=\frac{2}{\pi}\int_0^\infty B_{ij}(\omega)\cos\omega t\,d\omega\\&i,j=1,2,3,4,5,6\end{aligned} \tag{7}$$

Calculation of the damping terms are done according to the methodology of Kang (TBP) which is a 3-D unsteady potential theory method using a green function representing a translating pulsating source therefore taking speed effects into account.

## 3. EXPERIMENTAL STUDIES

### 3.1 Steady Force Measurements with Fully Constrained Model.

Implementation of the dynamic forces will be through a database obtained from experiments. In a low-encounter frequency environment the problem is very close to steady problem therefore it can be assumed that the dynamic forces the craft is going to be subject to will also act like steady. Experiments to systematically measure the steady forces acting on the hull of a semi-displacement craft (Figure 2) were carried out[1]. The model was attached to a 6 degrees of freedom load-cell and constrained in predefined positions to measure the forces acting on the hull. The test matrix is given in Table 1 where the sign convention is the same as the numerical model.

Table1 Test Matrix

| Fn | 0.4 | 0.5 | 0.6 | 0.7 | 0.8 |
|---|---|---|---|---|---|
| Trim (degrees) | +2 | +1 | 0 | -2 | -4 |
| Sinkage (mm) | +20 | +10 | 0 | -10 | -20 |

The forces measured are $F_z$, which is the force component in vertical direction, $F_x$, which is the force component in the direction of the carriage movement and $M_y$, which is the moment around the center of gravity in vertical direction. The load-cell is calibrated to measure the forces around the center of gravity and the model setup is set in such a way that the rotations are around center of gravity and the sway, roll and yaw motions are restrained completely and the sinkage and trim can be set manually. The resultant forces due to carriage speed are only dynamic components as the load-cell is set to zero before each run.

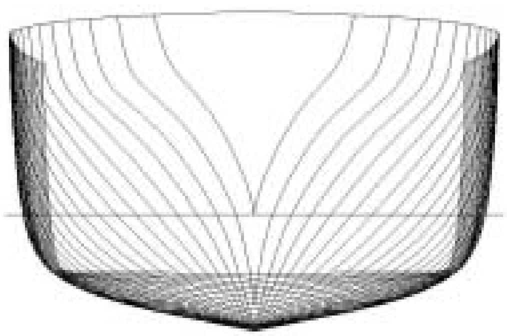

Figure 2. TC-60 Lines Plan

[1] Test were performed at
The Center for Marine Hydrodynamics
Acre Road, Glasgow, UK, G20 OTL

Table 2. TC-60 Principal Particulars

| | |
|---|---|
| $L_{OA}$ (m) | 1.000 |
| $L_{WL}$ (m) | 0.950 |
| B (m) | 0.166 |
| T (m) | 0.044 |
| $C_B$ | 0.542 |
| $C_M$ | 0.734 |
| $C_P$ | 0.738 |
| Wetted Surface ($m^2$) | 0.159 |
| $\Delta$ (N) | 34.923 |

Because of spray limitations especially at bow-down trim angles with high sinkage values, some tests are immeasurable, hence the total number of tests performed are 98 instead of the proposed 125 cases. The results of the tests are summarized in Figures 3 to 8. The effect of change of sinkage and speed for constant trim angle are shown for Dynamic Lift Force, which is defined as the force component acting normal to keel, and Trim Moment around the center of gravity.

The results are open to discussion since there was no time to run consistency tests. The force changes almost linearly as the sinkage is decreased from negative to positive for a single speed and trim is increased bow-up. As speed increases significant trim moment occurs after Froude number 0.4. A certain relationship between sinkage and bow-down trim with force and moment could not be established because spray generated at higher speeds made it difficult to get a healthy measurement. The results seem to generally agree with each other and are consistent with Ikeda et. al. (1993) and Ikeda, Katayama and Okumura (2000).

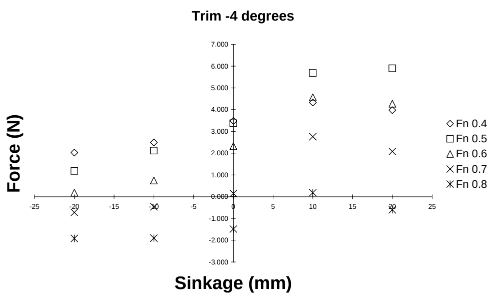


Figure 3. Change of Lift (-4 degrees trim)

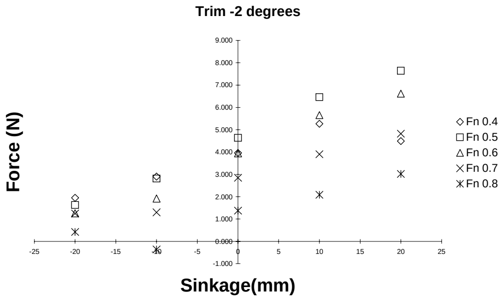


Figure 4. Change of Lift (-2 degrees trim)

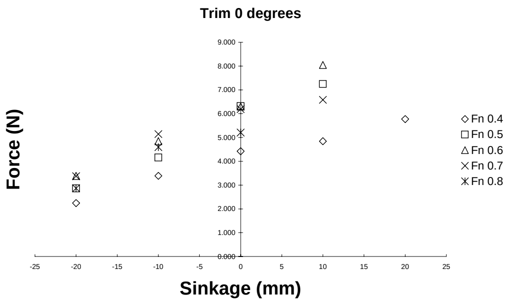


Figure 5. Change of Lift (0 degrees trim)

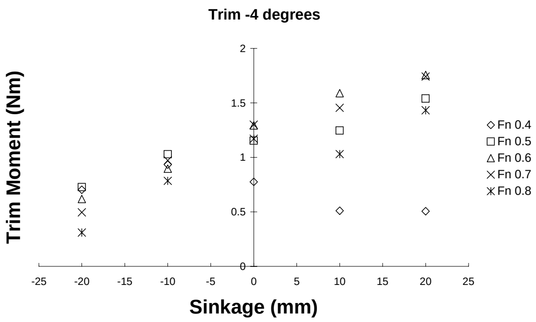


Figure 6. Change of  Moment (-4 degrees trim)

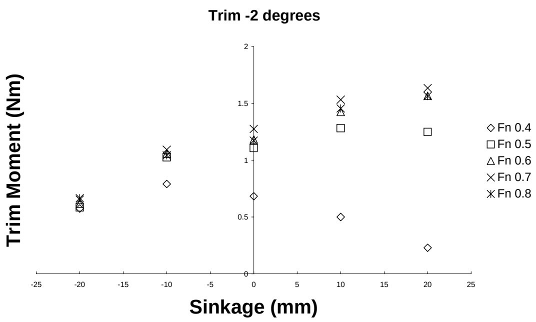


Figure 7. Change of Moment (-2 degrees trim)

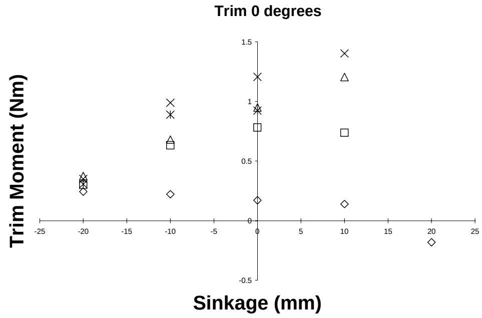


Figure 8. Change of Moment (0 degrees trim)

### 3.2 Seakeeping Experiments with Semi-captive Model Tests.

Motion response of the craft for regular waves at following seas was tested for differing wave conditions and hull speeds in order to validate the applicability of the numerical tool. The model was attached to the carriage and was free to heave and pitch motions only. This setup by definition ignores surge coupling and therefore numerical simulations were performed considering this effect. Table 2 presents the tested wave frequencies and Froude numbers.

Table3.Cases for Seakeeping Experiments

| ω / Fn | 3.502 | 4.530 | 5.548 | 6.410 | 7.835 |
|---|---|---|---|---|---|
| 0.4 | X | X | X | X | X |
| 0.6 | X | X | X | - | - |
| 0.7 | - | - | X | X | X |
| 0.8 | X | X | X | - | - |

Experimental results are compared to numerical results using the database approach initially. It was observed that results obtained using this method gives insufficient results in both motions even for low speeds as seen in Figures 9 and 10.

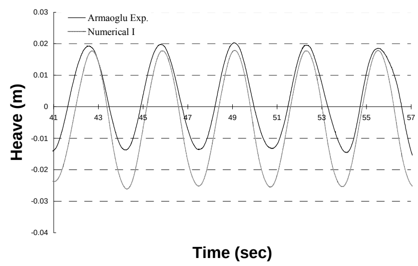


Figure 9. Heave Motion ω=3.502 Fn=0.4

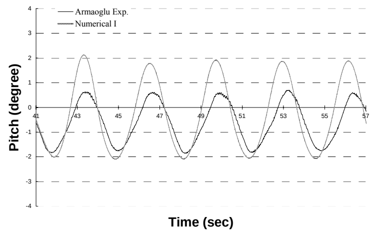

Figure 10. Pitch Motion ω=3.502 Fn=0.4

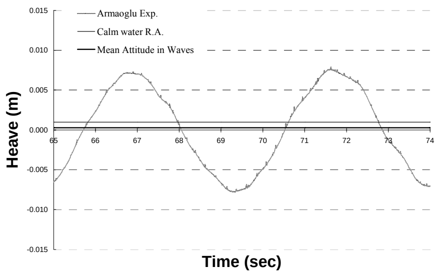

Figure 11. Mean Attitude in Heave ω=5.548 Fn=0.7

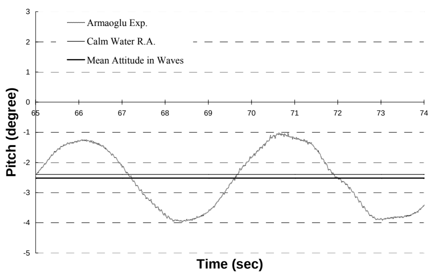

Figure 12. Mean Attitude in Pitch ω=5.548 Fn=0.7

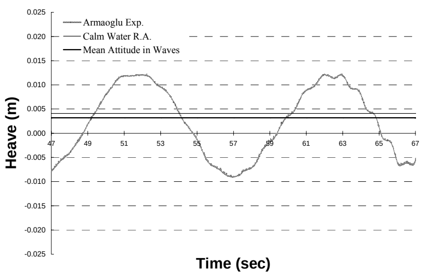

Figure 13. Mean Attitude in Heave ω=4.530 Fn=0.6

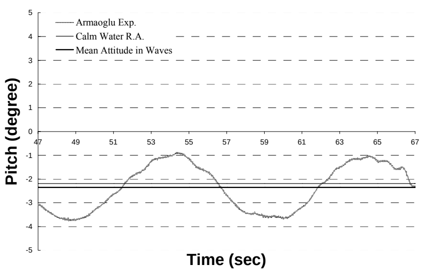

Figure 14. Mean Attitude in Pitch ω=4.530 Fn=0.6

In due process of analysing the seakeeping results it is seen that the mean attitude of the motions is very close to the running attitude in calm water regardless of the wave frequency. This might be because the planing pressures are not developed sufficiently and the static forces are still dominant. This is better seen in Figures 11 to 14. From these figures it is observed that the pitch moment in Figure 10 is not sufficiently high enough to bring the craft to the running attitude.

## 3.3 Roll Decay Tests

Roll decay tests were performed for four speed conditions including zero speed. The results and the comparison with numerical simulations are presented in the following figures. For higher speeds a deviation from the zero roll angle is seen at the model tests. This may be caused by the shifting of the weights used to properly ballast the model as the initial roll angle is quite big and the model beam is very small.

Roll damping is increased because of speed and the effect can be seen from the reduced roll period in Fn 0.4. Roll period of Fn 0.6 is slightly

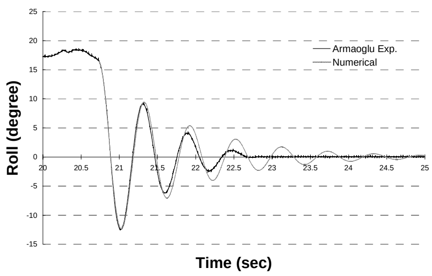

Figure 15. Roll Decay at Zero Speed

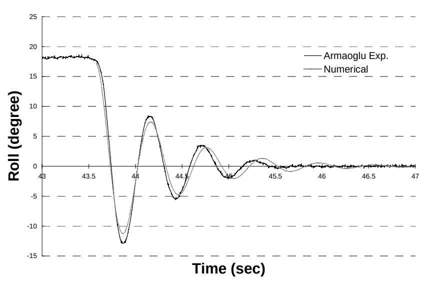

Figure 16. Roll Decay at Fn=0.4

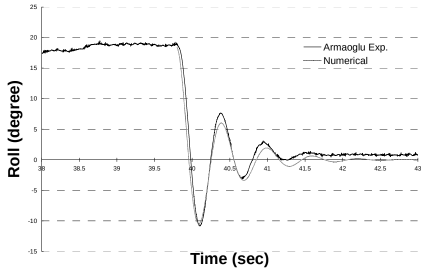


Figure 17. Roll Decay at Fn=0.6

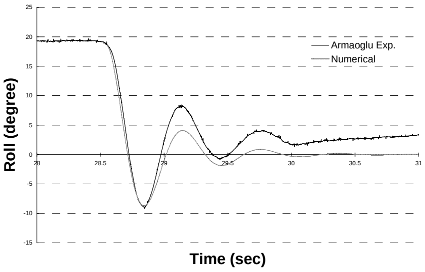


Figure 18. Roll Decay at Fn=0.8

higher than Fn 0.4. A possible reason for this is the running attitude's effect on rollrestoring moment or a tendency for unstable roll motion at this speed. In Fn 0.8, the roll period and the number of oscillations and the amplitude of a cycle are reduced. The roll period reduction clearly shows the increase of roll damping due to speed meanwhile the reduction of the number of roll oscillations and amplitude of a cycle shows the increased roll restoring moment because of the dynamic lift. The change in roll period is shown in Table 4.

Table 4 Change of Roll Period with Speed

| *Froude Number* | *Roll Period (sec)* |
|---|---|
| 0.0 | 0.909 |
| 0.4 | 0.550 |
| 0.6 | 0.625 |
| 0.8 | 0.267 |

## 4. VALIDATION OF THE NUMERICAL RESULTS

From the observations of seakeeping experiments as mentioned in 3.2 a different approach will be implemented to include the effect of dynamic forces to the model. This will be the assumption that the calm water running attitude is equal to the mean running attitude in waves for this speed range. This assumption although very simple, is applicable to initial design stage and is very fast, omitting the overcomplicated (thus prone to error) database approach. The results are presented in Figures 19-23. In Figures 19 and 20 heave amplitude is slightly overestimated and pitch amplitude slightly underestimated. This shows the importance of using correct damping coefficients taking speed effects into account. The effect of running attitude is reflected correctly with the mean attitude assumption. Figures 21 and 22 shows even better agreement with the experiments with higher speeds for different modes of motion. It is seen that our assumption is valid in this speed range and numerical results are well within engineering limits however calculation of hydrodynamic coefficients must be handled properly.

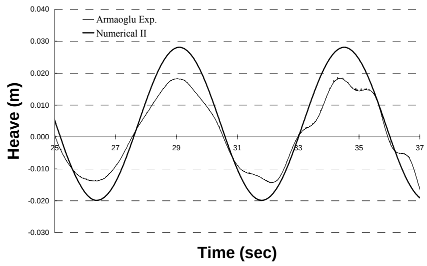


Figure 19. Heave Motion ω=3.502 Fn=0.6

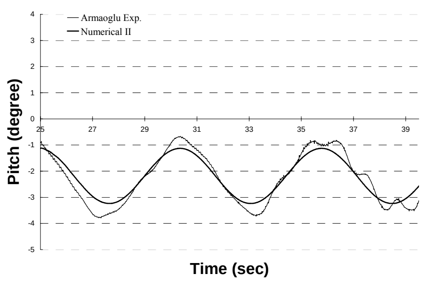


Figure 20. Pitch Motion ω=3.502 Fn=0.6

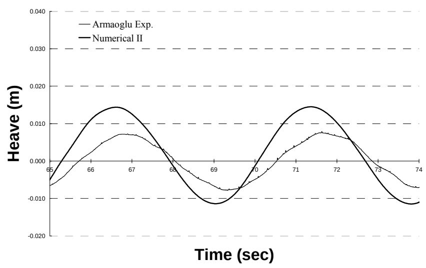


Figure 21. Heave Motion ω=3.502 Fn=0.8

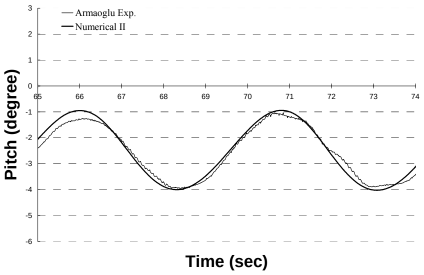

Figure 22. Pitch Motion ω=5.548 Fn=0.7

## 5. EFFECT OF RUNNING ATTITUDE ON TRANSVERSE STABILITY

In general practice GZ curve is used to assess the intact transverse stability of a HSC. Calculations in IMO HSC Code are performed at the design waterline which corresponds to the maximum operational weight of the craft with no lift or propulsion machinery active. Roll and pitch stability is qualitatively assessed during safety trials and operational restrictions may be imposed according to the results. This however tells very little in initial design stage of how the actual stability is affected because of speed. If it is assumed that the running attitude of the craft is the actual balance condition of the craft for a given speed, then GZ curve calculations can be performed in this balance condition for relatively small roll angles assuming that the speed loss due to roll angle is negligible. In Figure 23 it is clearly seen that running attitude alone reduces the transverse stability of the craft by reducing the lever arm even for small angles of roll.

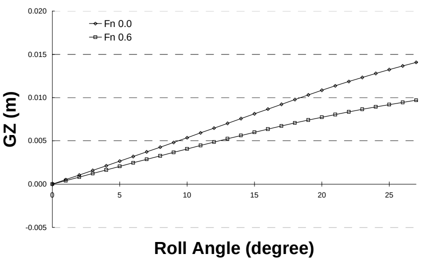

Figure 23. Effect of Speed on GZ Curve

Further reduction to this effect will be imposed in waves and also because of weather conditions. Although the roll damping characteristics are increased because of speed, if the righting arm lever is negative for a given roll angle, this will not prevent the craft from capsizing. This also shows that evaluating intact stability of HSC on static design criteria is insufficient. Therefore, applying performance based criteria would be the way forward for robust and accurate transverse-stability analysis of semi-displacement craft. A detailed effort applying this approach is currently being carried out following validation analysis presented herein.

## 6. CONCLUSIONS

Several aspects of the effect of speed on semi-displacement ships are investigated. Experiments were performed to verify the results produced by the numerical tool. Following conclusions were obtained:

For low encounter frequencies the dynamic forces can be assumed to act steady.

Database approach to evaluate the dynamic forces is over-engineered and prone to error in this speed range. The assumption that the mean running attitude in waves is equal to the calm water running attitude is valid.

The effect of roll motion on vertical dynamic forces is not taken into account however roll-pitch coupling is achieved via non-linear restoring calculation in mathematical model.

Running attitude alone causes reduction in transverse stability. Combined with further reduction in waves and wind this might lead to dangerous situations.

Even the small analysis of the effect of speed on transverse stability herein indicate that the static criteria might be insufficient to evaluate High Speed Craft characteristics. Performance based criteria imposed on early design stage could be a good way forward to assess stability thoroughly and safety based design.

## 7. REFERENCES


Ayaz, Z., 2003, "Manoeuvring Behaviour of Ships in Extreme Astern Seas." PhD Thesis, University of Strathclyde, Glasgow, UK

Ayaz, Z., Vassalos, D., Spyrou, K.J., & Matsuda, A., 2002, "Towards a Six Degrees of Freedom Manoeuvring Mathematical Model in Random Seas." In: Proceedings of the Sixth International Workshop on Stability and Operational Safety of Ships, Webb Institute, New York, USA.

Ayaz, Z., Vassalos, D., & Turan, O., 2006, "Parametric Studies of a new numerical model for controlled ship motions in extreme astern seas" Journal of Marine Science and Technology, Vol. 11, No. 1, pp.19-38.

Baba, E., Asai, S., & Toki, N., 1982, "A Simulation Study on Sway-Roll-Yaw Coupled Instability of Semi-Displacement Type High Speed Craft." In: Proceedings of the Second International Conference on Stability of Ships and Ocean Vehicles., pp. 79-90.

Bailey, D., 1976, "The NPL High Speed Round Bilge Displacement Hull Series." Maritime Technology Monograph, No. 4.

Codega, L., & Lewis, J., 1987, "A Case Study of Dynamic Instability in a Planing Hull." Marine Technology, Vol. 24 (2), pp. 143-163.

Cummins, W. E., 1962, "The Impulse-Response Function and Ship Motions." Schiffstechnik, Vol. 47, pp.101-109.

De Kat, J.O., & Paulling, J.R., 1989, "The Simulation of Ship Motions and Capsizing in Severe Seas." Transactions of the Society of Naval Architects and Marine Engineers, Vol. 97, pp.139-168.

Hamamoto, M., & Kim, Y., 1993, "A New Coordinate System and the Equations Describing Manoeuvring Motion of a Ship in Waves." Journal of the Society of Naval Architectures of Japan, Vol. 173, pp. 209-220.

Ikeda, Y., Katayama, T., & Okumura, H., 2000, "Characteristics of Hydrodynamic Derivatives in Manoeuvring Equations for Super High Speed Planing Hulls." In: Proceedings of the 10th International Offshore and Polar Engineering Conference, Vol. 4, pp. 434-444. Seattle, USA.

Ikeda, Y., Yokomizo, K., Hamasaki, J., Umeda, N., & Katayama, T., 1993, "Simulation of Running Attitude and Resistance of a High-Speed Craft Using a Database of Hydrodynamic Forces Obtained by Fully Captive Model Experiments." In: The 7$^{th}$ International Conference on Fast Sea Transportation., pp. 583-594.

IMO, 2000, International Code of Safety for High-Speed Craft, Publisher: International Maritime Organization, London, UK.

ITTC, 1999, "The Specialist Committee on Stability." Final Report and Recommendations to the 22$^{nd}$ ITTC. In: Proceedings of the 22$^{nd}$ ITTC, Seoul and Shanghai. Retrieved May , 23, 2006. from: http://ittc.sname.org/proceedings.htm

ITTC, 2002, "The Specialist Committee on Prediction of Extreme Ship Motions and Capsizing." Final Report and Recommendations to the 23$^{rd}$ ITTC. In: Proceedings of the 23$^{rd}$ ITTC, Vol 2, Venice, Italy., pp. 611-657.

Katayama, T., 2002, "Experimental Techniques to Assess Dynamic Instability of High-Speed Craft - Non-zero Heel, Bow-Diving, Porpoising and Transverse Porpoising." In: Proceedings of the Sixth International Ship Stability Workshop. Glen Cove, New York, USA.

Kang. J., (To Be Published), "Time Domain Mathematical Model for Manoeuvring Simulation in a Wave", PhD Thesis, University of Strathclyde, Glasgow, UK.

Martin, M., 1978, "Theoretical Determination of Porpoising Instability of High-Speed Planing Boats." Journal of Ship Research, Vol. 22 (1), pp. 32-53.

Marwood, W.J., & Bailey, D., 1968, "Transverse Stability of Round-Bottomed High Speed Craft Underway." National Physics Laboratory, Ship Report N°. 98.

BMT SeaTech Limited, 2003, "High Speed Craft in Following and Stern Quartering Seas: Report on Phase 1 of MCA Research Study 502", Project No: C3423. Retrieved May , 22, 2006. from: http://www.mcga.gov.uk/c4mca/research_report_502_phase_1.pdf

Ohkusu, M, 1986, "Prediction of Wave Forces on a Ship Running in Following Waves with Very Low Encountered Frequency." Journal of Society of Naval Architects of Japan, Vol. 159, pp. 129-138.

Ritter, O.K & Templeman M.T., 1998, "High-Speed Sealift Technology" Total Ship Systems Engineering Directorate Technology Projection Report, Carderock Division Naval Surface Warfare Center, USA. Retrieved March , 19, 2004. from: http://www.ccdott.org/hss_volume2/01_hss_workshop_tech.pdf

Von Karman, T., 1929, "The Impact of Seaplane Floats During Landing." NACA TN N°.321.

Yegorov, I., Bun'Kov, M., & Sadovnikov, Y. M., 1981, "Propulsive Performance and Seaworthiness of Planing Vessels." NAVSEA Translation N°. 1965. Washington D.C., USA.

Yeh, H. Y. H., 1965, "Series 64 Resistance Experiments on High-Speed Displacement Forms." Marine Technology, Vol. 2, pp. 248-272.